

Crystallography based investigation of weak interaction for drug designing against COVID-19

Nayim Sepay,^{*a,b} Pranab Saha,^a Zarrin Shahzadi,^b Aratrika Chakraborty^b and Umesh Chandra Halder^{*a}

^aDepartment of Chemistry, Jadavpur University, Kolkata 700 032, India

^bDepartment of Chemistry, Lady Brabourne College, Kolkata 700 017, India.

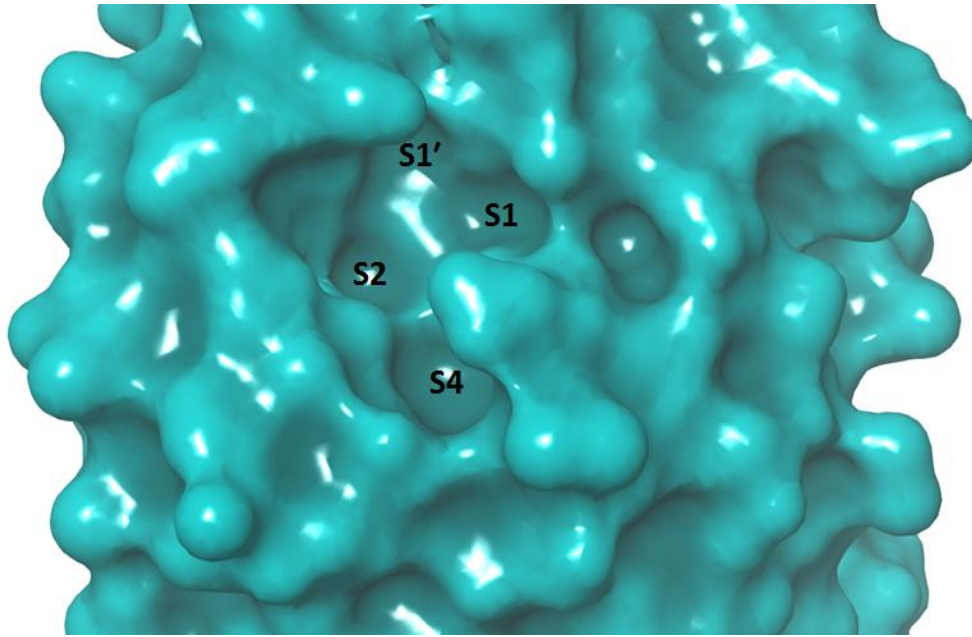


Figure S1: The major domains inside the active site of SARS-CoV-2 M^{pro} protein

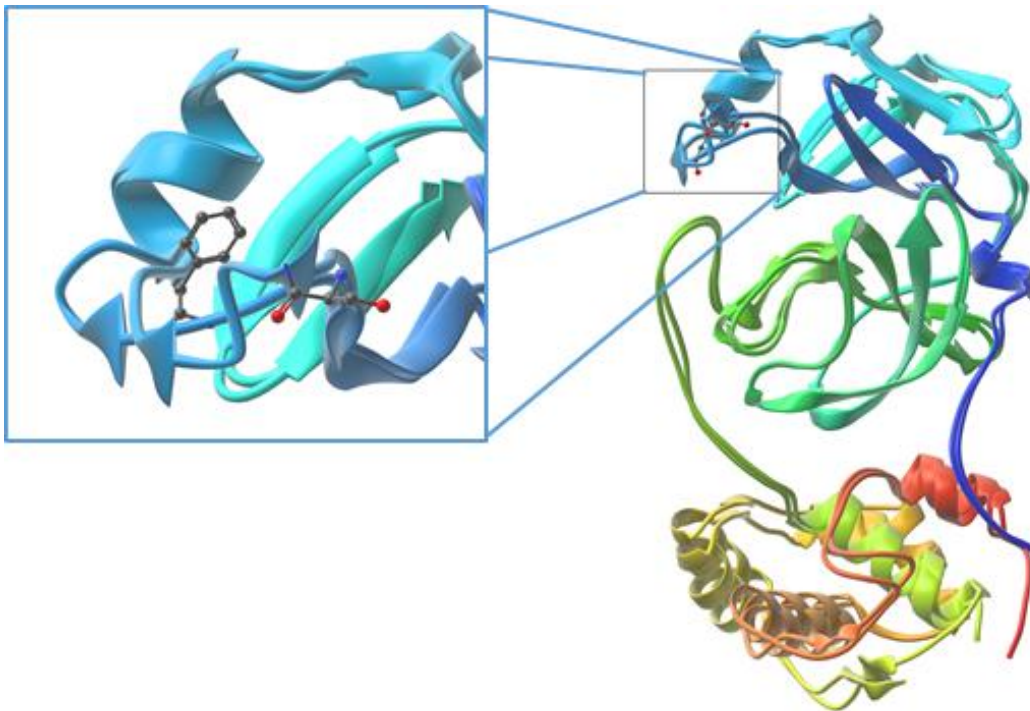


Figure S2: The mutation of amino acid 46 of SARS-CoV M^{pro} with Ser residue was found at the active site of SARS-CoV-2 M^{pro} (PDB ids of SARS-CoV M^{pro} and SARS-CoV-2 M^{pro} is 1P9S and 6LU7).

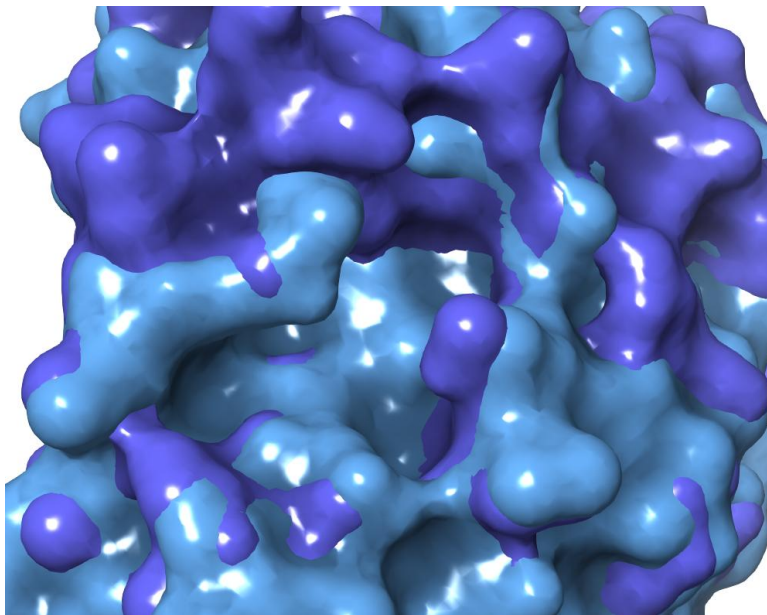


Figure S3: The change of depth and size of the active site of SARS-CoV-2 M^{pro} for the mutation (PDB ids of SARS-CoV M^{pro} and SARS-CoV-2 M^{pro} is 1P9S and 6LU7).

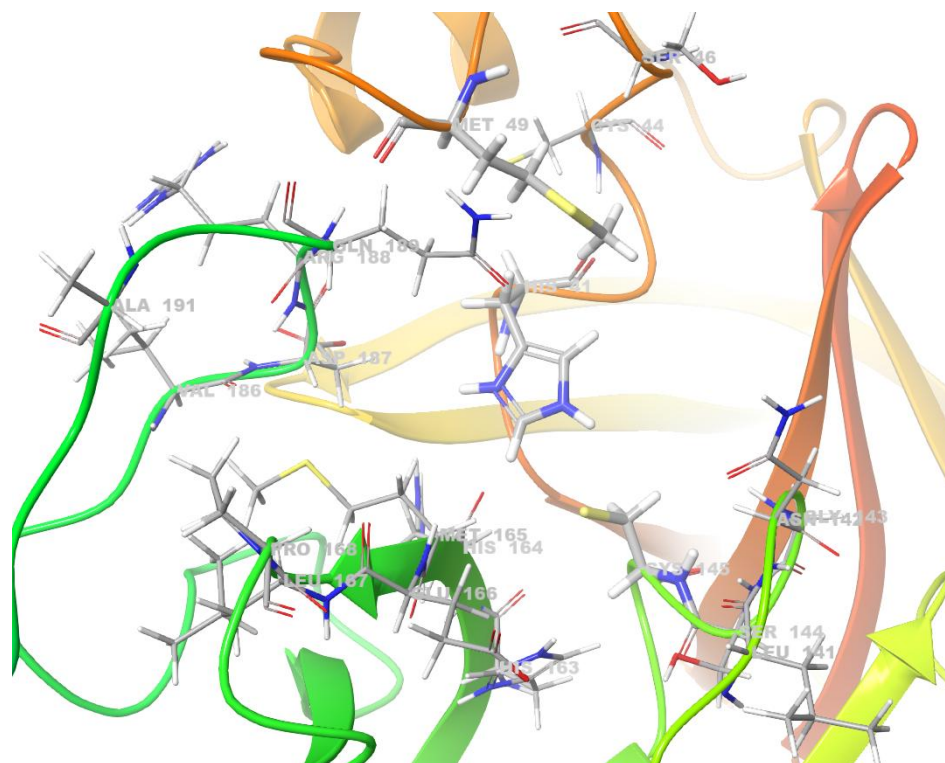
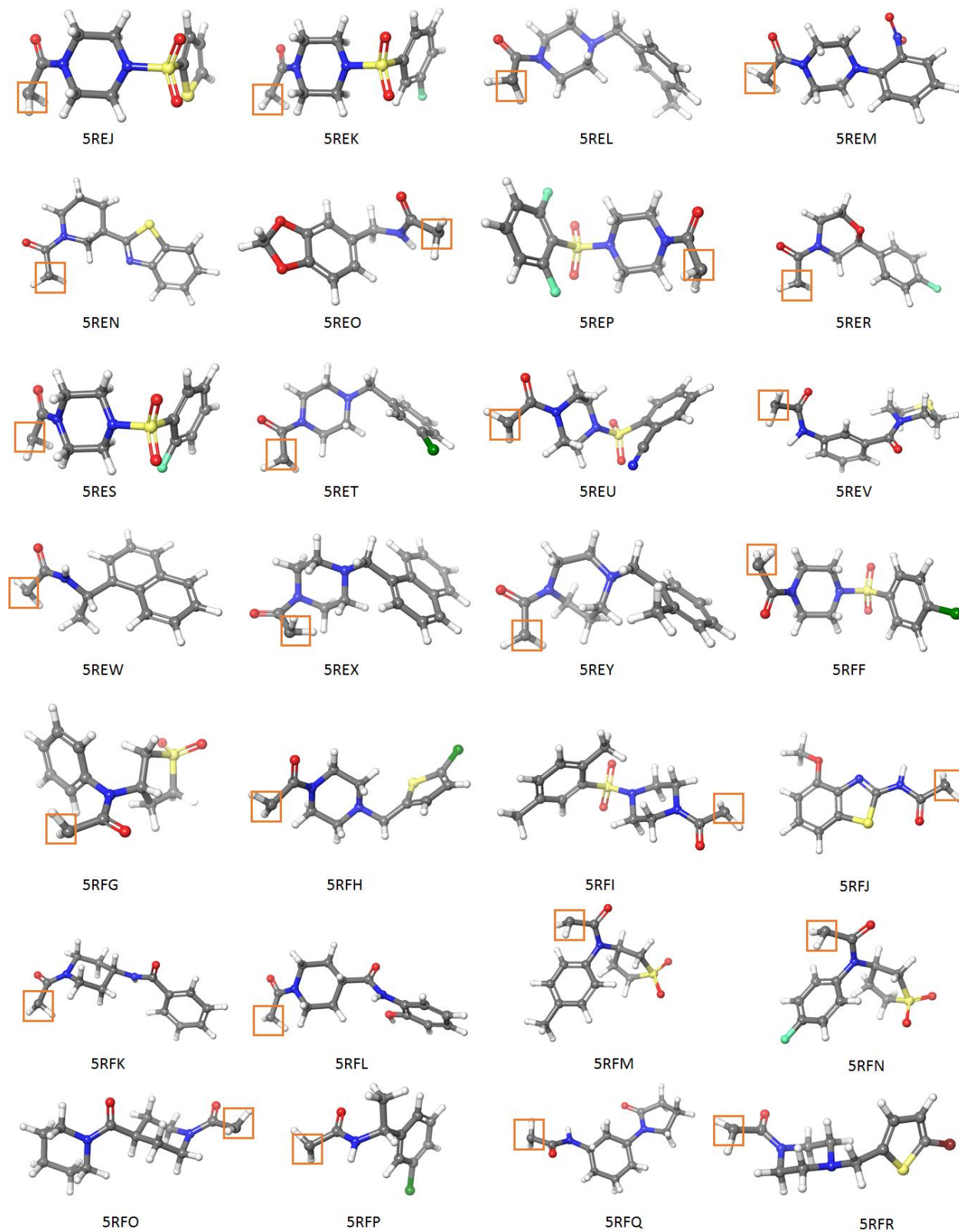
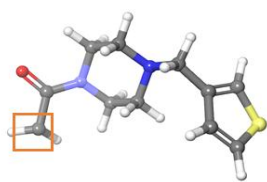


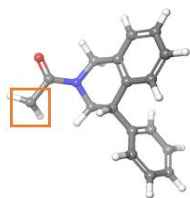
Figure S4: The constituent amino acid residues of SARS-CoV-2 M^{pro}.

Covalently attached small molecules

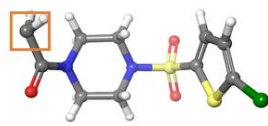




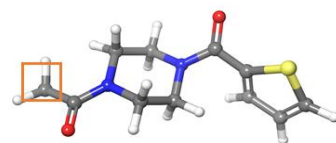
5RFS



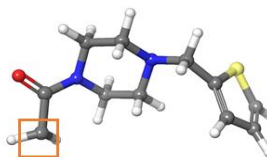
5RET



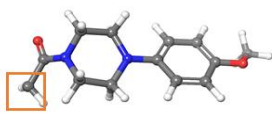
5REU



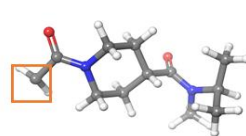
5REV



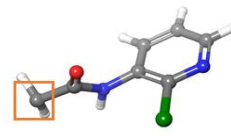
5RFW



5RFX



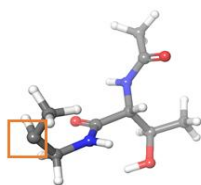
5RFY



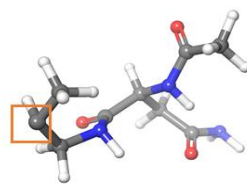
5RFZ



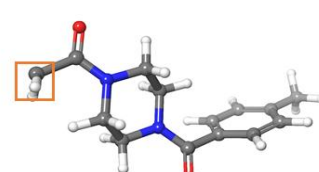
5RGO



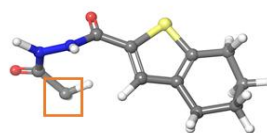
5RG2



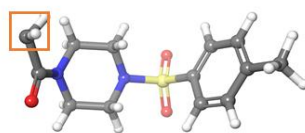
5RG3



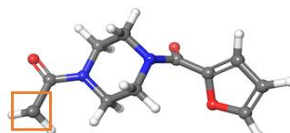
5RGL



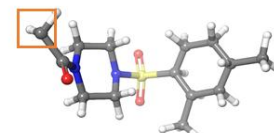
5RGM



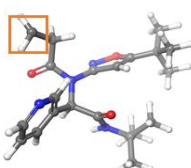
5RGN



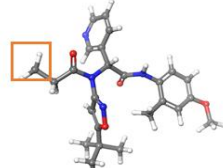
5RGO



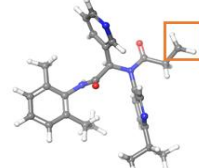
5RGP



5RGT



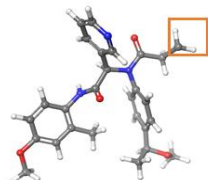
5RH5



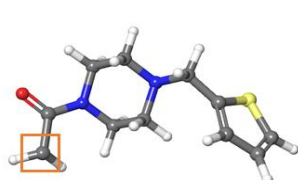
5RH6



5RH7



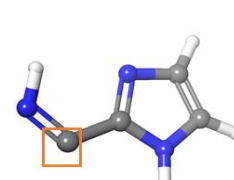
5RH9



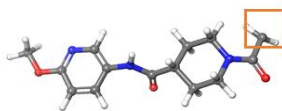
5RHA



5RHB



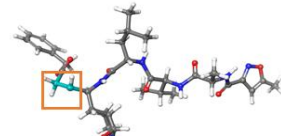
5RHC



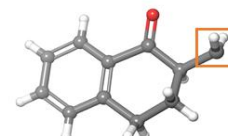
5RHE



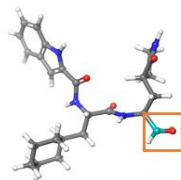
5RHF



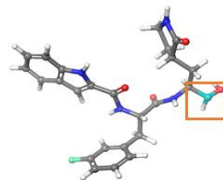
6LU7



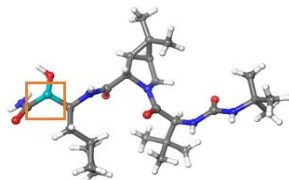
6YNQ



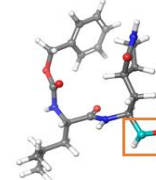
6LZE



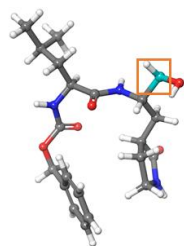
6MOK



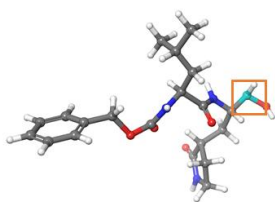
6WNP



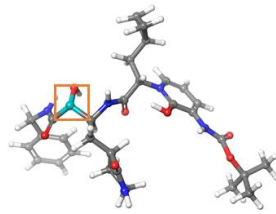
6WTJ



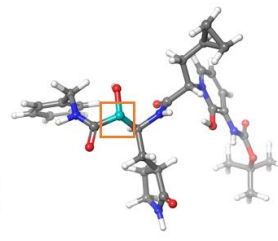
6WTK



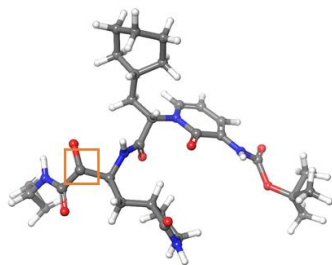
6WTM



6Y2F



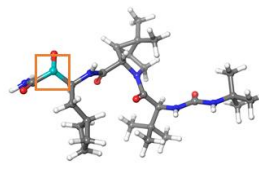
6Y2G



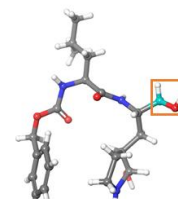
6Y7M



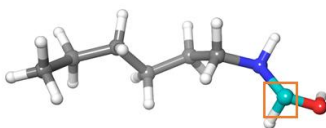
7BQY



7BRP

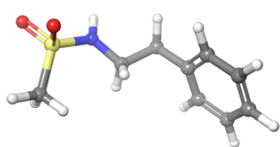


7BRR

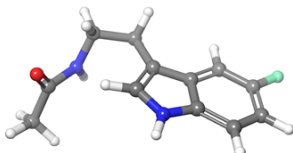


7BUY

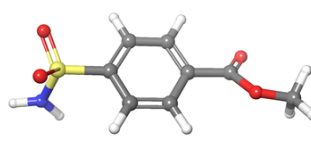
Non-covalently attached small molecules



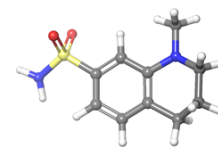
5R7Y



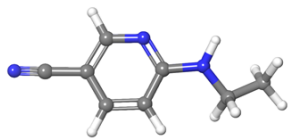
5R7Z



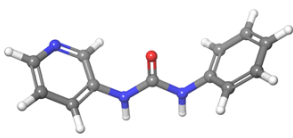
5R80



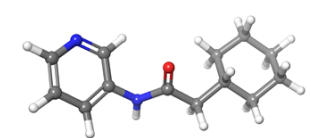
5R81



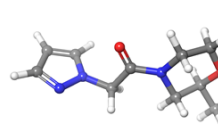
5R82



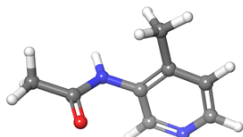
5R83



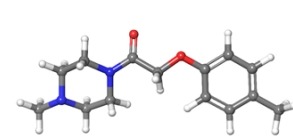
5R84



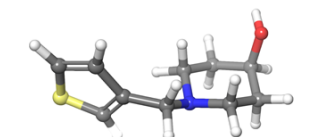
5R89



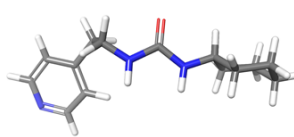
5RE4



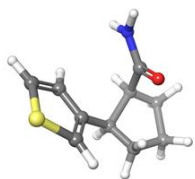
5RE9



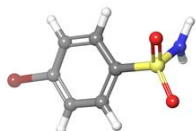
5REB



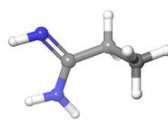
5REH



5REZ



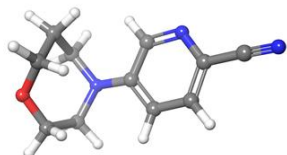
5RF1



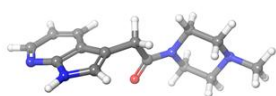
5RF2



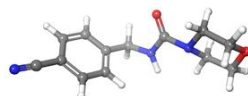
5RF3



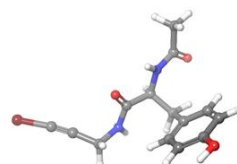
5RF6



5RF7



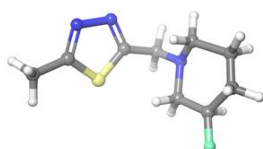
5REE



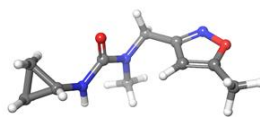
5RG1



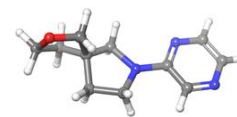
5RGG



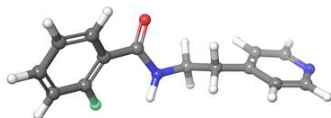
5RGH



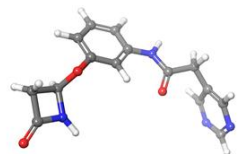
5RGI



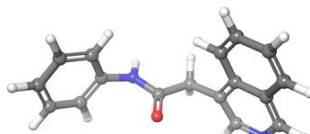
5RGJ



5RGK



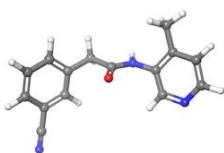
5RGU



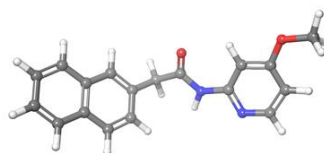
5RGV



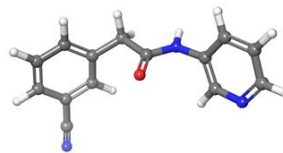
5RGW



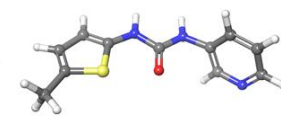
5RGX



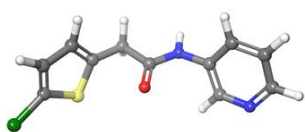
5RGY



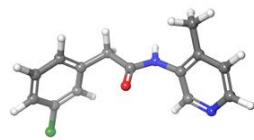
5RGZ



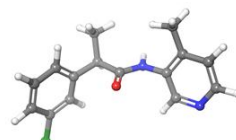
5RH0



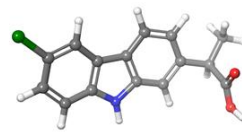
5RH1



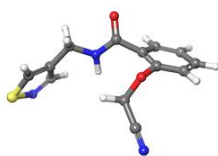
5RH2



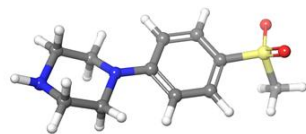
5RH3



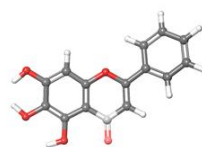
5RH4



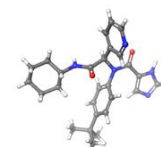
5RH8



5RHD



6M2N



6W63

Small molecules attached non-covalently at outside of the active side

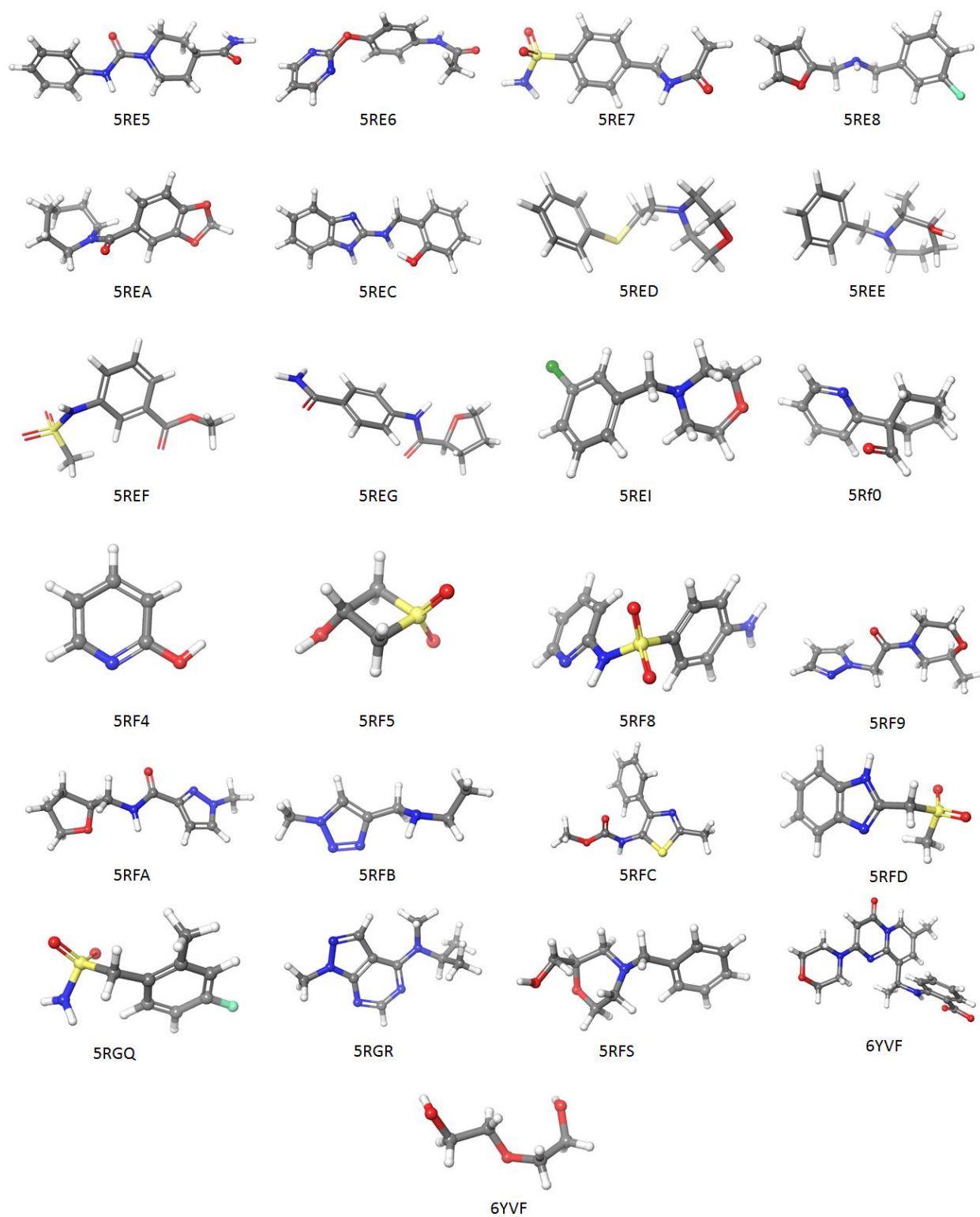


Figure S5: Small molecules found in the SARS CoV-2 M^{PRO} protein crystal as a bound ligand through different binding modes.



Figure S6: Distribution of small molecule ligand around the SARS-CoV-2 M^{pro} enzyme.

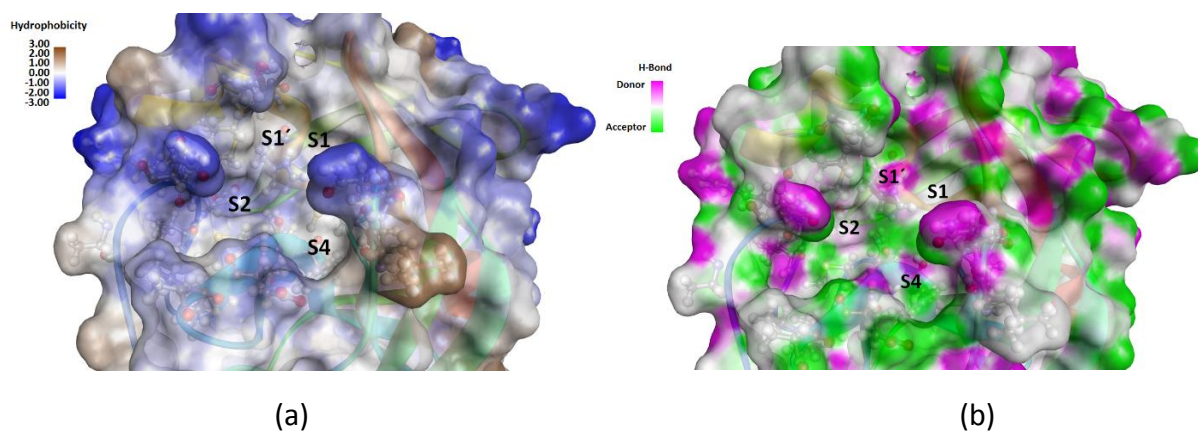


Figure S7: The map of (a) hydrophobicity-hydrophilicity and (b) hydrogen bond donor-acceptor regions in the active site of the SARS-CoV-2 M^{pro} protein.

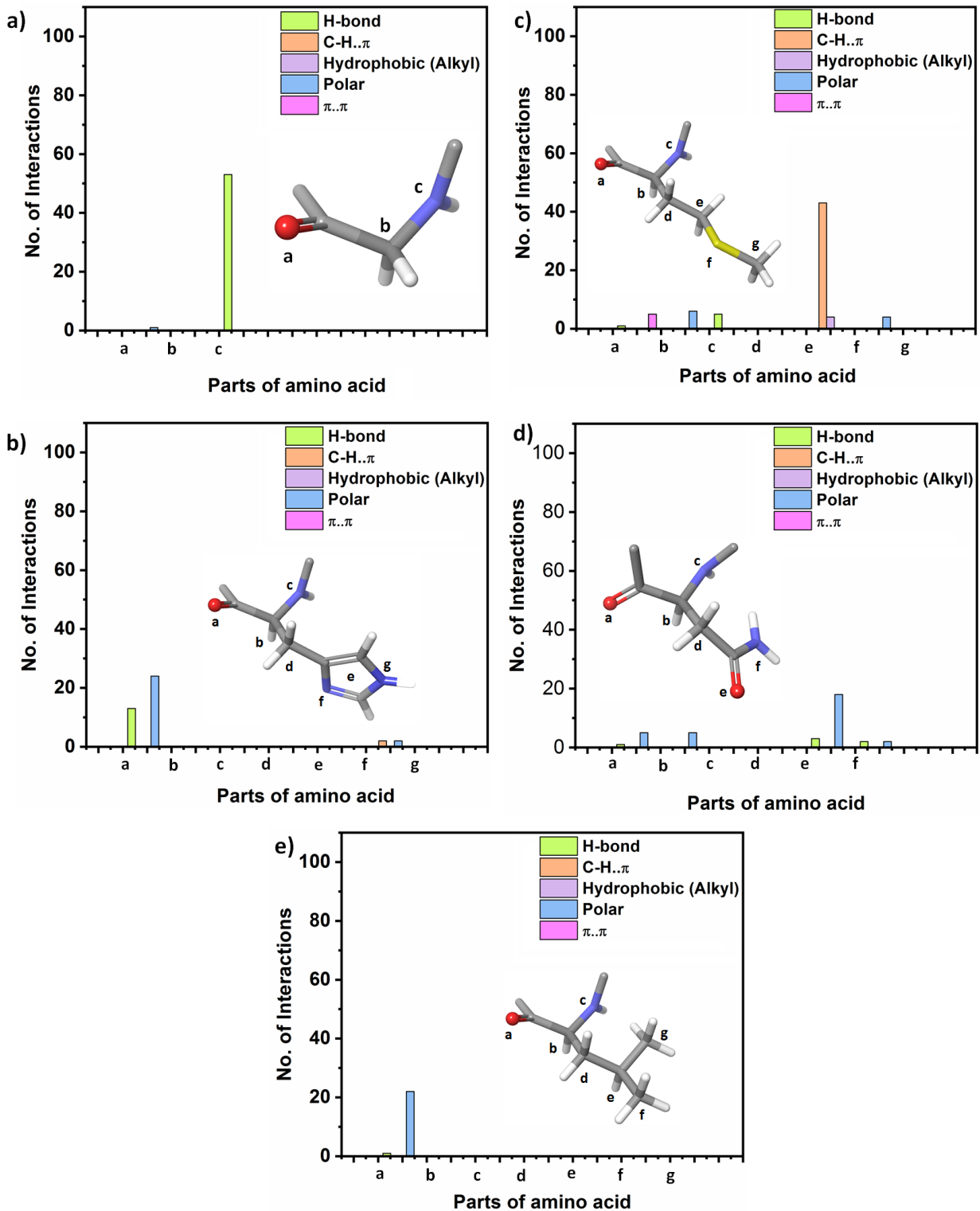


Figure S8: In the active site of the SARS-CoV-2 M^{PRO} enzyme, the population of H-bond, C-H... π , hydrophobic, polar and π ... π interactions at different parts of (a) G143; (b) G143, (c) M165, (d) N142 and (e) L141 amino acids.

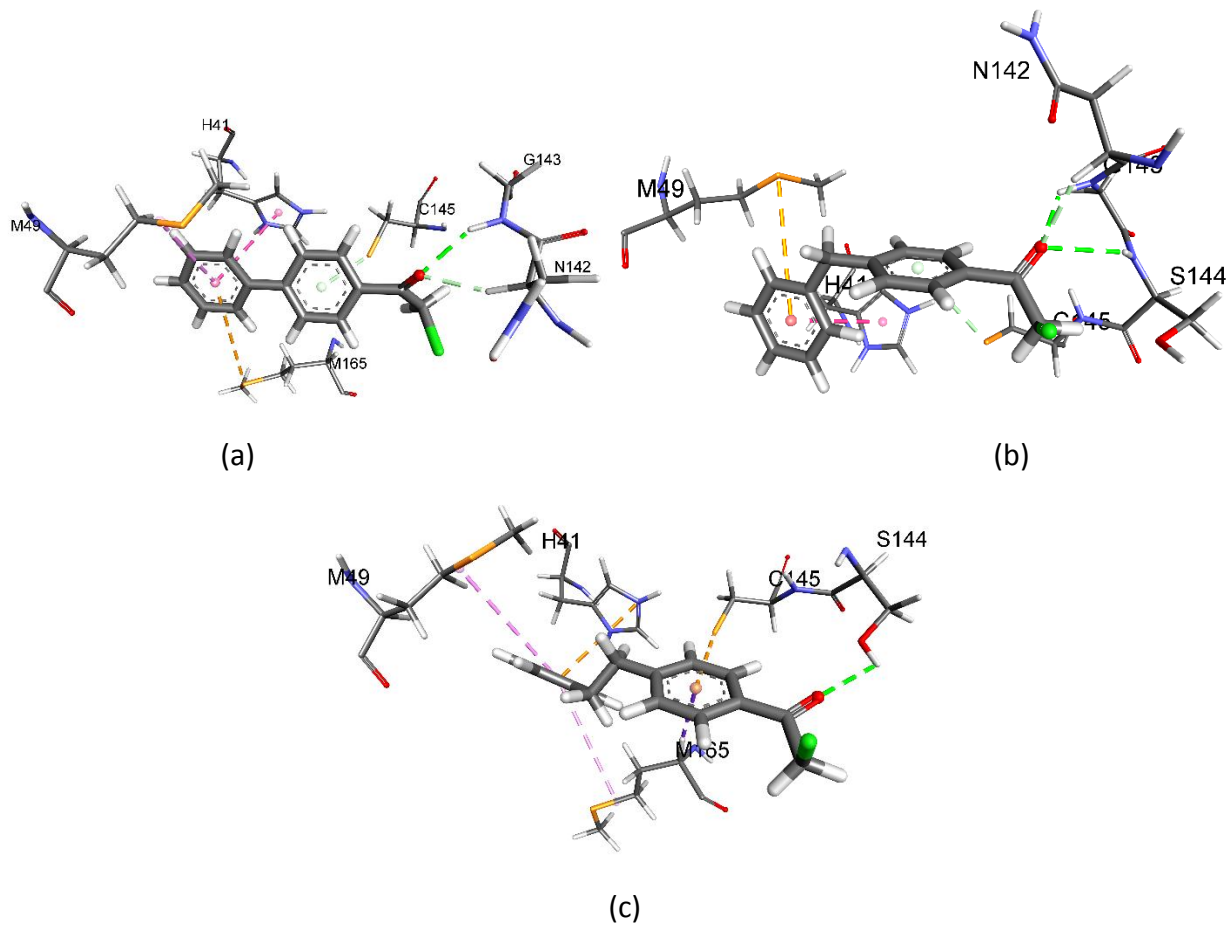
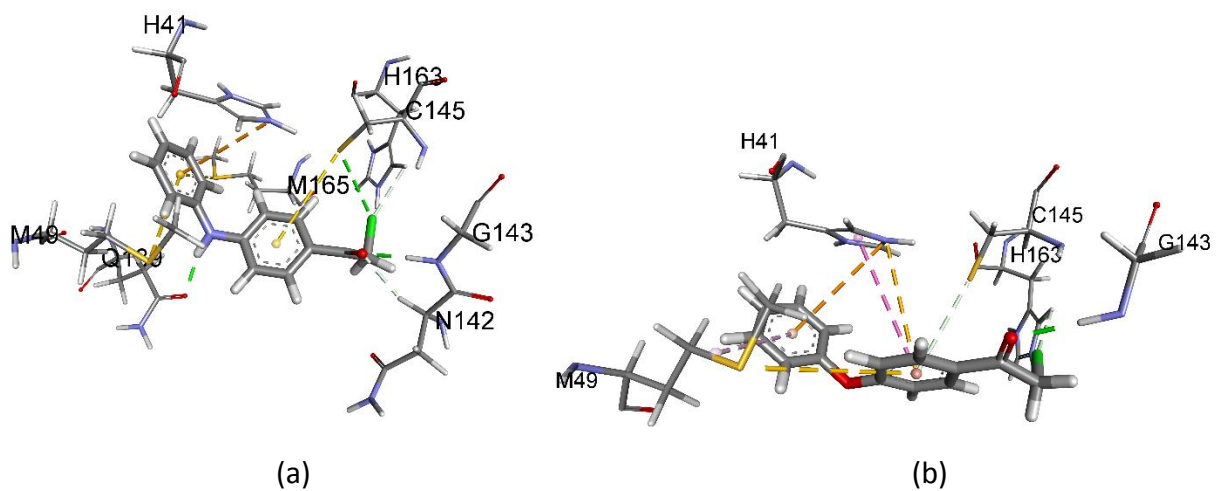


Figure 9: Non-covalent interactions of (a) compound 1, (b) compound 2 and (c) compound 3 inside the active site of SARS-CoV-2 M^{pro} enzyme.



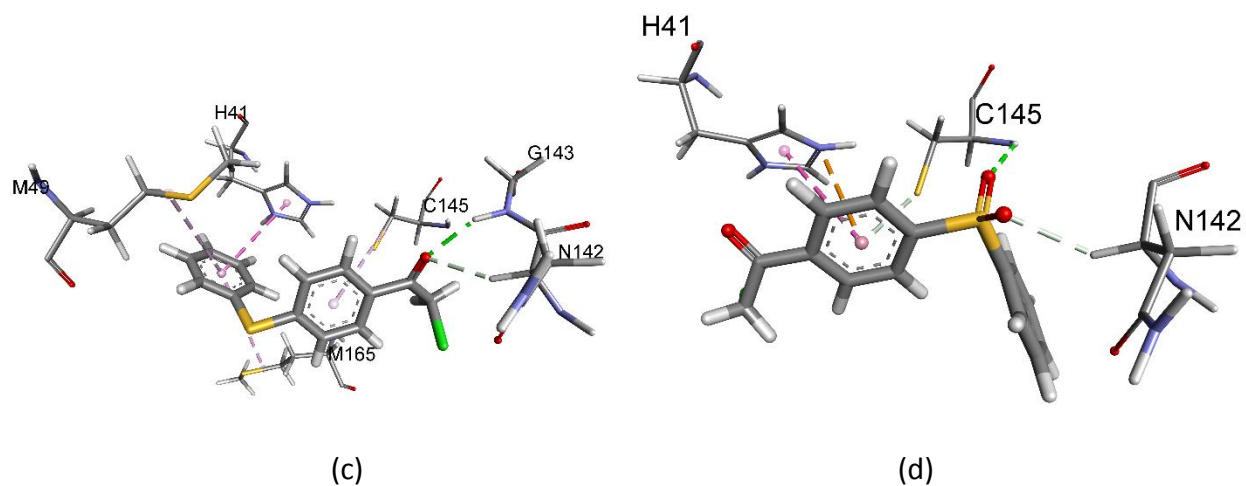


Fig. S10: Non-covalent interactions of (a) compound **4**, (b) compound **5**, (c) compound **6** and (d) compound **7** inside the active site of SARS-CoV-2 M^{pro} enzyme.

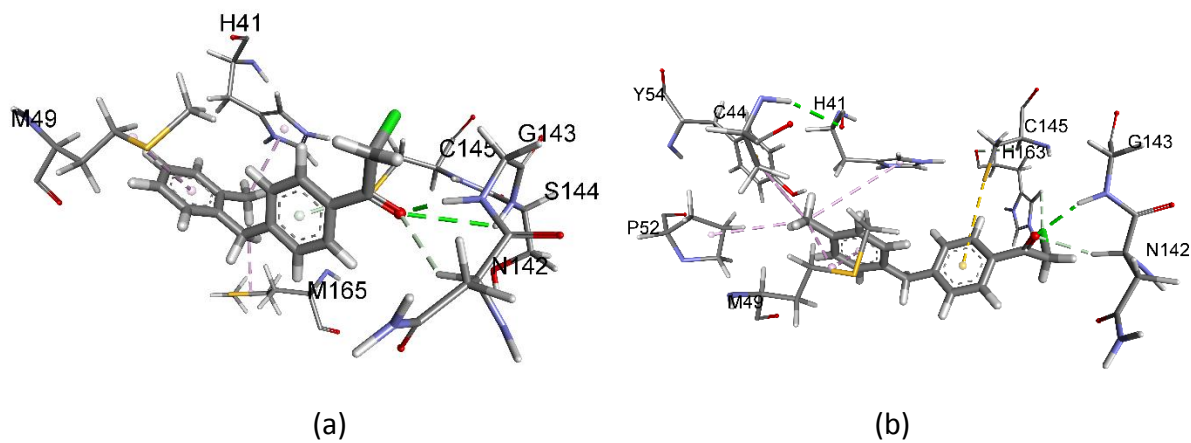


Fig. S11: Non-covalent interactions of (a) compound **8** and (b) compound **10** inside the active site of SARS-CoV-2 M^{pro} enzyme.

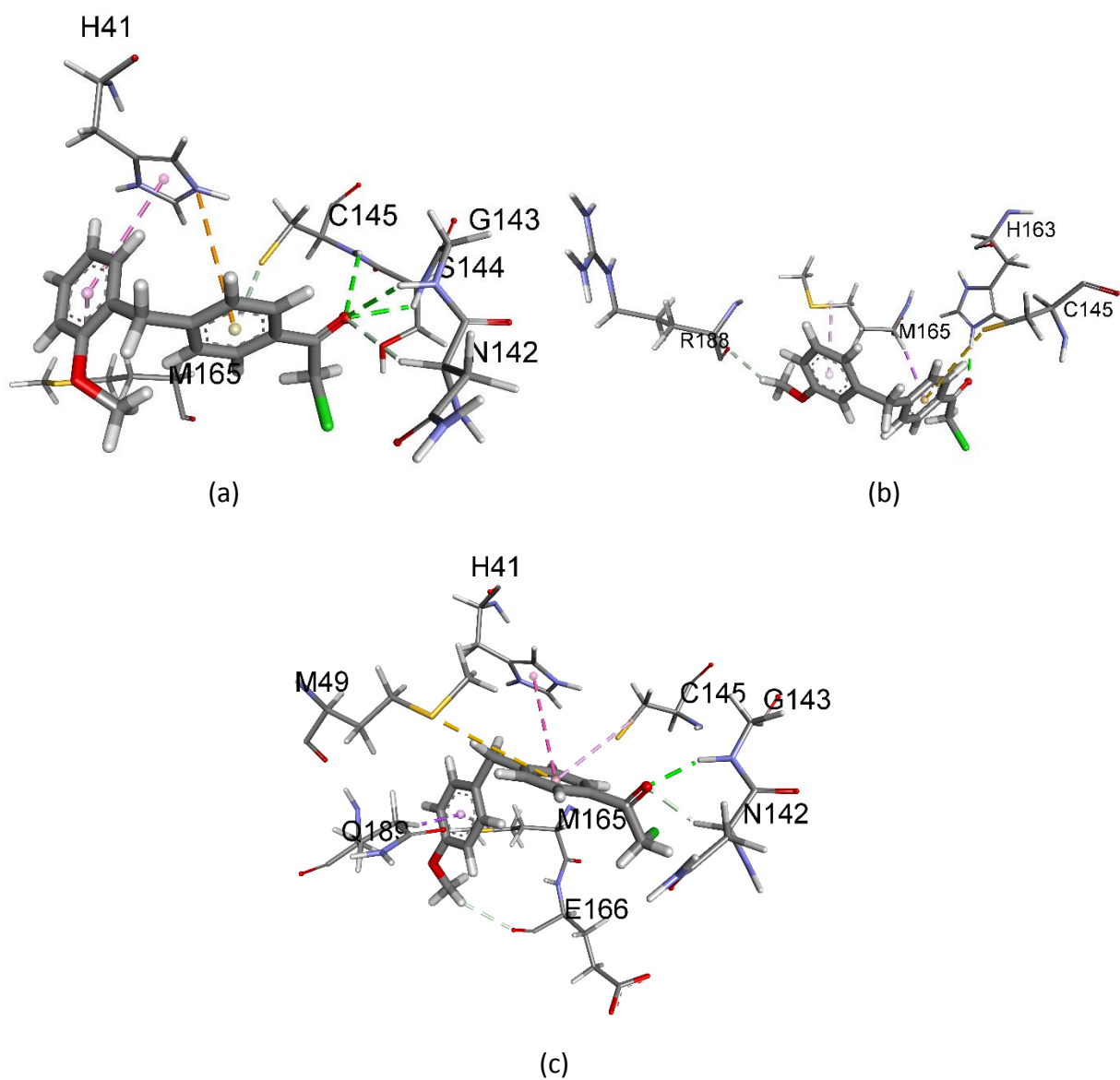


Fig. S12: Non-covalent interactions of (a) compound **11**, (b) compound **12** and (c) compound **13** inside the active site of SARS-CoV-2 M^{pro} enzyme.

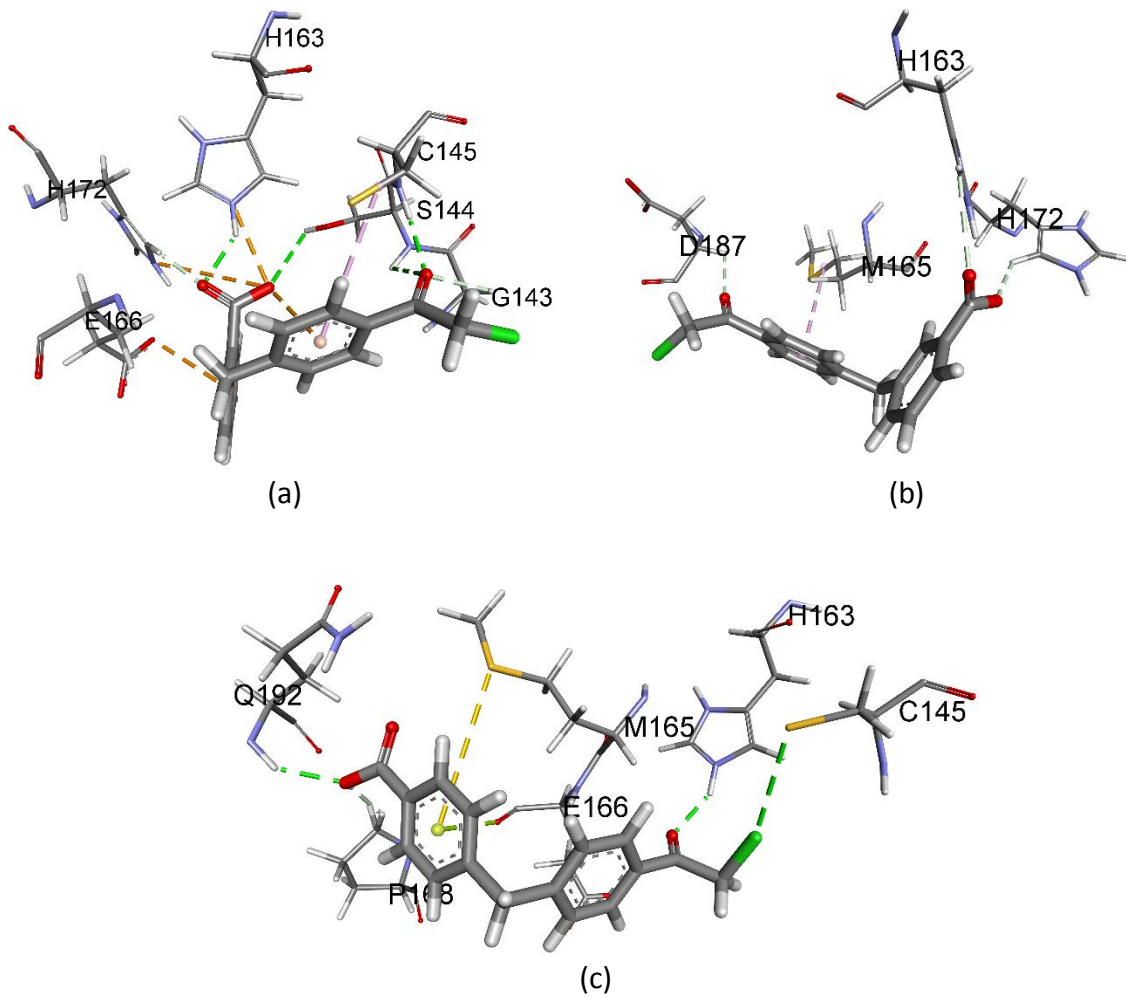


Fig. S13: Non-covalent interactions of (a) compound **14**, (b) compound **15** and (c) compound **16** inside the active site of SARS-CoV-2 M^{pro} enzyme.

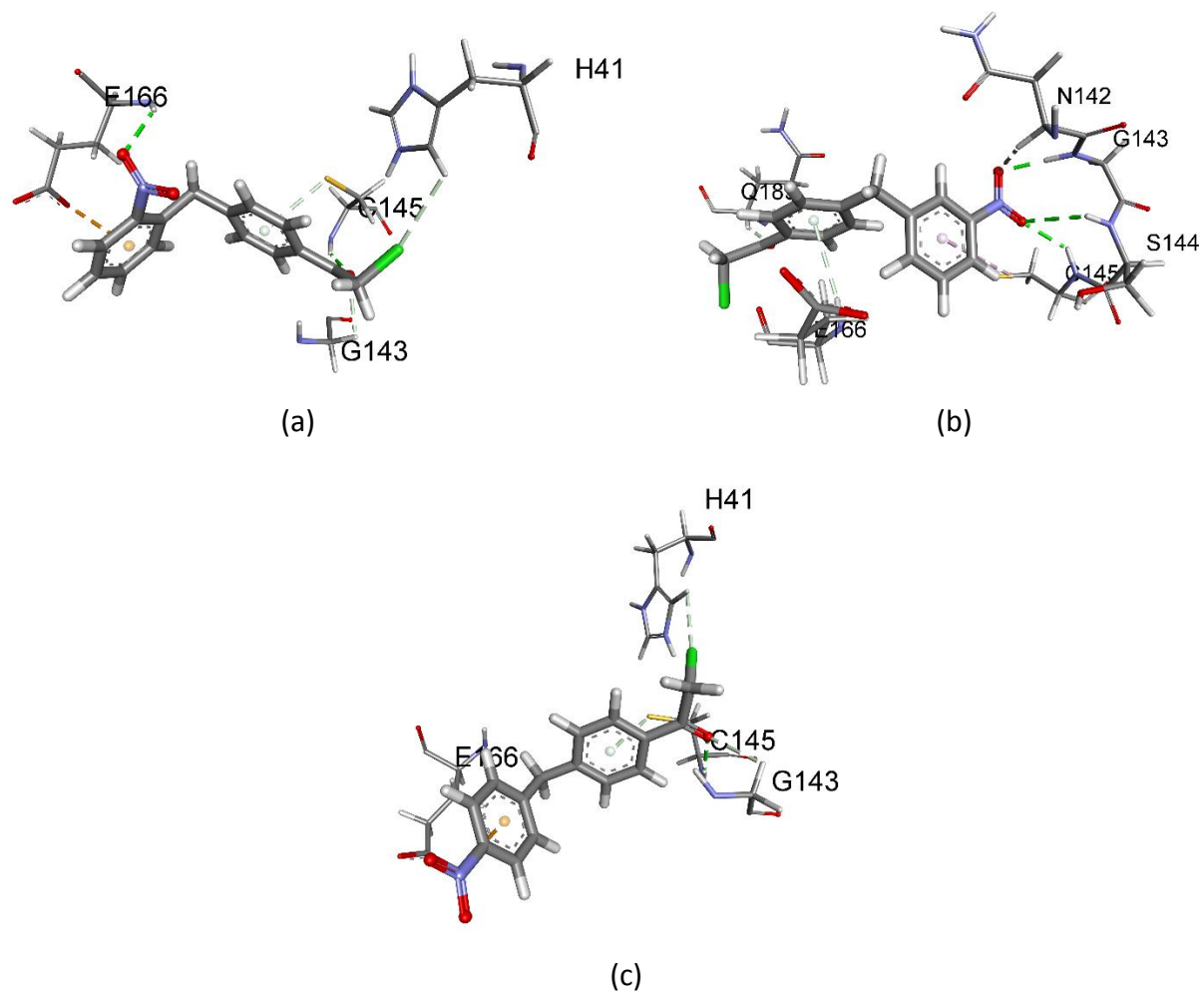


Fig. S14: Non-covalent interactions of (a) compound **17**, (b) compound **18** and (c) compound **19** inside the active site of SARS-CoV-2 M^{pro} enzyme.

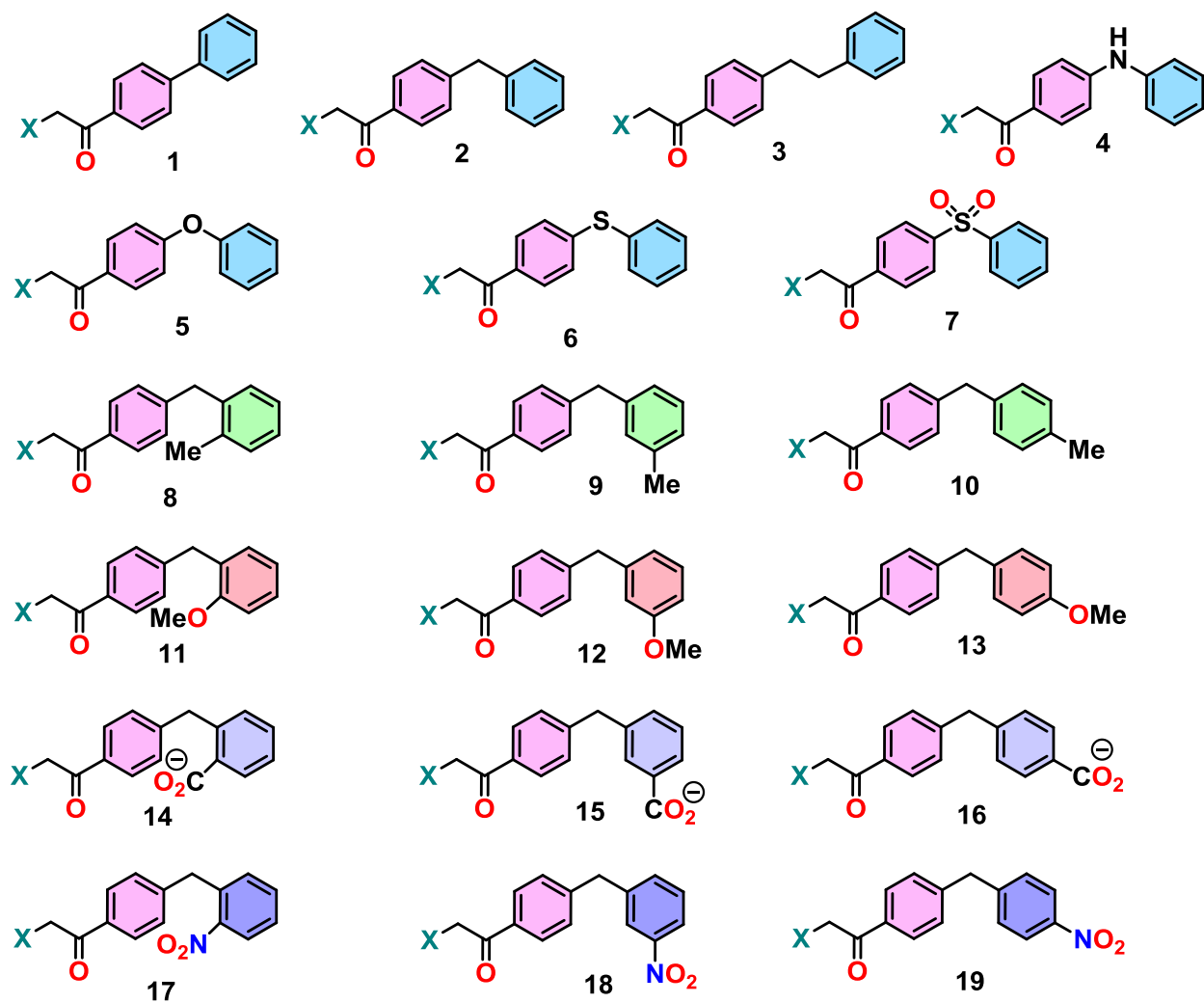
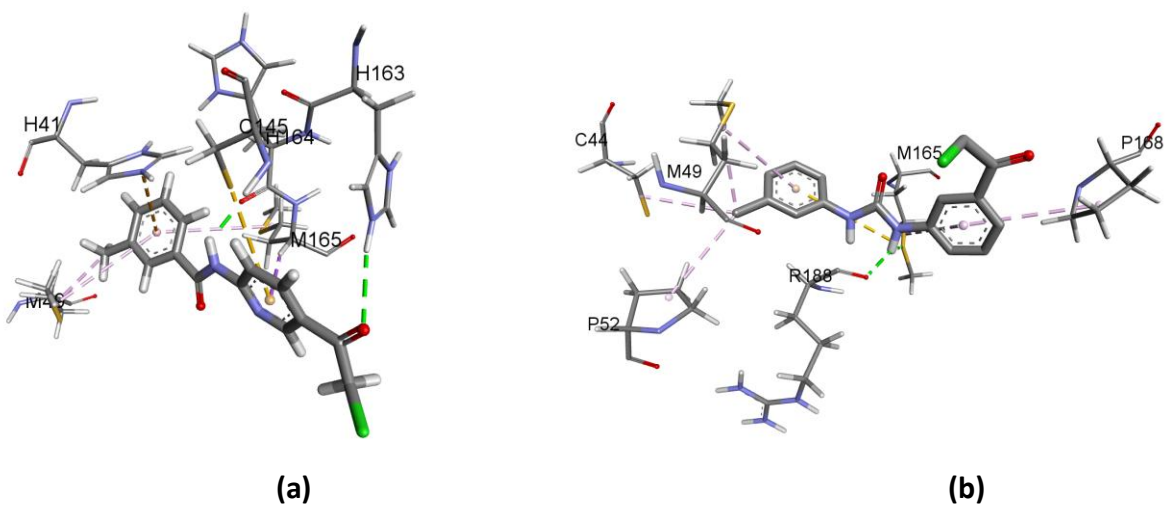


Fig. S15: 2D chemical structure of the designed compound.



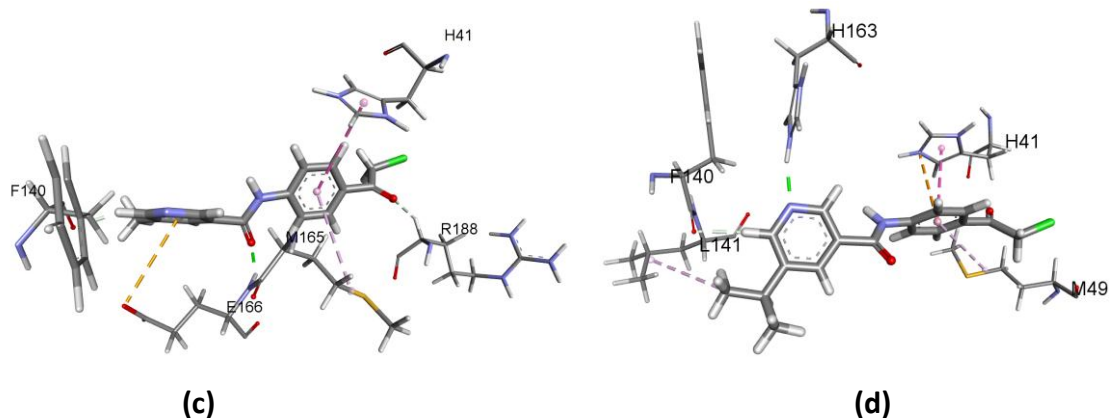


Fig. S16: Non-covalent interactions of (a) compound **21**, (b) compound **22**, (c) compound **23** and (d) compound **24** inside the active site of SARS-CoV-2 M^{pro} enzyme.

Table S1. PDB IDs of SARS-CoV-2 M^{pro} enzyme

Position of Small molecules		PDB ID
No Small molecules (apo)		5R8T, 6M2Q, 6M03, 6WQF, 6WTM, 6Y2E, 6Y84, 6Y87, 7BRO.
Outside of the active site		5RE5, 5RE6, 5RE7, 5RE8, 5REA, 5REC, 5RED, 5REE, 5REF, 5REG, 5RF1, 5RF4, 5RF5, 5RF8, 5RF9, 5RFA, 5RFB, 5RFC, 5RFD, 5RGQ, 5RGR, 5RGS, 6VYF.
Inside of the active site	Covalently attached	5REJ, 5REK, 5REL, 5REM, 5REN, 5REO, 5REP, 5RER, 5RES, 5RET, 5REU, 5REV, 5REW, 5REX, 5REY, 5RFF, 5RFG, 5RFH, 5RFI, 5RFJ, 5RFK, 5RFL, 5RFM, 5RFN, 5RFO, 5RFP, 5RFQ, 5RFR, 5RFS, 5RET, 5REU, 5REV, 5RFW, 5RFX, 5RFY, 5RFZ, 5RG0, 5RG2, 5RG3, 5RGL, 5RGM, 5RGN, 5RGO, 5RGP, 5RGT, 5RH5, 5RH6, 5RH7, 5RH9, 5RHA, 5RHB, 5RHC, 5RHE, 5RHF, 6LU7, 6QMQ, 6LXE, 6MOK, 6WNP, 6WTJ, 6WTK, 6WTM, 6Y2F, 6Y2G, 6Y7M, 7BQY, 7BRP, 7BRR, 7BUY.
	Non-covalently attached	5R7Y, 5R7Z, 5R80, 5R81, 5R82, 5R83, 5R84, 5R89, 5RE4, 5RE9, 5REB, 5REH, 5REZ, 5RF1, 5RF2, 5RF3, 5RF6, 5RF7, 5REE, 5RG1, 5RG2, 5RG3, 5RG4, 5RG8, 5RHD, 6M2N, 6W63.

Table S2. The p-values for testing the difference between each of amino acids

	H41	C145	M49	G143	E166	M165	H164	N142	L141	S144	C44	P168	Q189	H163	R188	A 191	S46	L167	V 186	D187	
H41																					
C145	0.063																				
M49	0.00049	0.0375																			
G143	1.9E-09	5E-06	0.0034																		
E166	1.1E-09	3E-06	0.0026	0.4614																	
M165	4E-14	6E-10	5E-06	0.0374	0.0459																
H164	0	2E-12	5E-08	0.003	0.004	0.1626															
N142	0	3E-14	1E-08	0.0013	0.0018	0.1056	0.3947														
L141	0	5E-14	8E-10	0.0002	0.0003	0.0354	0.2027	0.286													
S144	0	0	1E-14	5E-08	8E-08	9E-05	0.0022	0.0047	0.02												
C44	0	0	4E-15	2E-08	3E-08	4E-05	0.0012	0.0026	0.012	0.4137											
P168	0	0	4E-15	2E-08	3E-08	4E-05	0.0012	0.0026	0.012	0.4137	0.5										
Q189	0	0	4E-15	2E-08	3E-08	4E-05	0.0012	0.0026	0.012	0.4137	0.5	0.5									
H163	0	0	0	3E-10	5E-10	1E-06	5E-05	0.0001	8E-04	0.1126	0.1587	0.1587	0.1587								
R188	0	0	0	3E-11	4E-11	1E-07	7E-06	2E-05	1E-04	0.0354	0.0544	0.0544	0.0544	0.2637							
A 191	0	0	0	7E-12	1E-11	4E-08	2E-06	6E-06	4E-05	0.0163	0.0261	0.0261	0.0261	0.1587	0.3527						
S46	0	0	0	2E-12	3E-12	1E-08	6E-07	2E-06	1E-05	0.0063	0.0105	0.0105	0.0105	0.0787	0.2073	0.3274					
L167	0	0	0	2E-12	3E-12	1E-08	6E-07	2E-06	1E-05	0.0063	0.0105	0.0105	0.0105	0.0787	0.2073	0.3274	0.5				
V 186	0	0	0	2E-12	3E-12	1E-08	6E-07	2E-06	1E-05	0.0063	0.0105	0.0105	0.0105	0.0787	0.2073	0.3274	0.5	0.5			
D187	0	0	0	2E-12	3E-12	1E-08	6E-07	2E-06	1E-05	0.0063	0.0105	0.0105	0.0105	0.0787	0.2073	0.3274	0.5	0.5	0.5		

Method of calculations

Group	1	2
Sample Size	N_1	N_2
Number of Events	X_1	X_2
Event Rate	λ_1	λ_2
Distribution of X	Poisson(λ_1)	Poisson(λ_2)

Mathews (2010) proposed two test statistics that can be used to test statistical hypotheses about the rate difference. The first is based on the *large-sample z-test* of the hypotheses $H_0: \lambda_1 = \lambda_2$ versus $H_a: \lambda_1 \neq \lambda_2$.

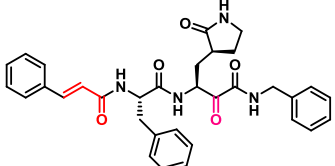
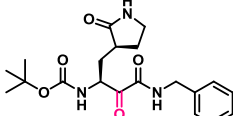
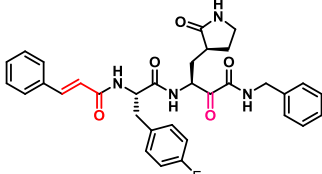
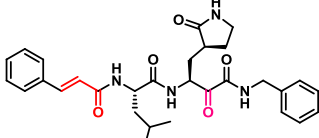
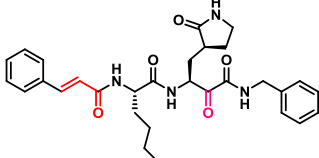
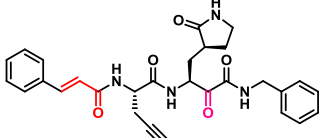
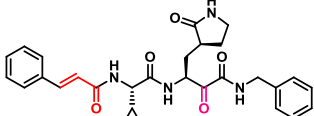
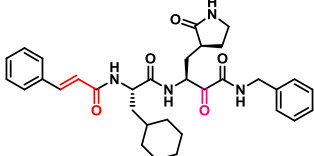
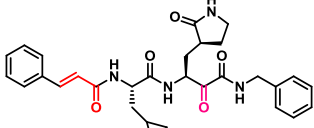
$$Z_{LS} = \frac{\lambda_2 - \lambda_1}{\sqrt{\frac{\lambda_1}{N_1} + \frac{\lambda_2}{N_2}}}$$

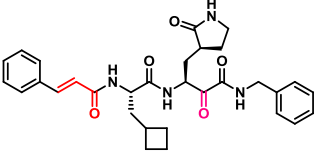
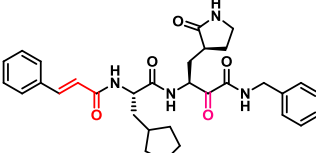
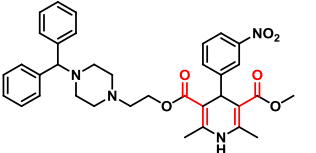
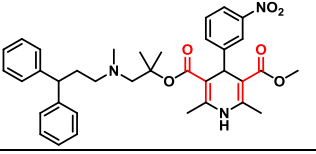
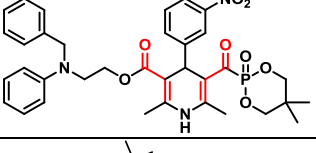
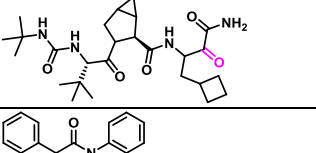
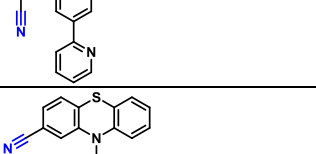
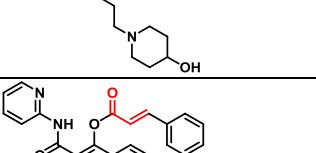
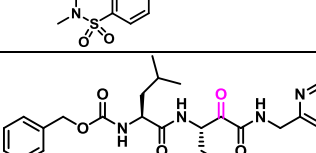
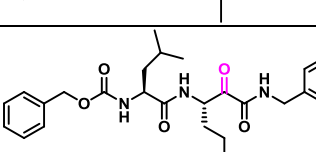
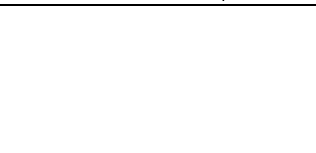
$p = P(Z > Z_{LS})$ Where Z follows N (0, 1)

Smith, P.G. and Morrow, R.H. 1996. *Field Trials of Health Intervention in Developing Countries: A Toolbox*. Macmillan Education. Oxford, England.

Campbell, M.J. and Walters, S.J. 2014. *How to Design, Analyze and Report Cluster Randomised Trials in Medicine and Health Related Research*. John Wiley. New York.

Table S3: Few examples of crystallographically non-characterized SARS-CoV-2 M^{pro} enzyme inhibitor small molecules

Entry	Structure of molecules	Reference
1		<i>J. Med. Chem.</i> 2020 , <i>63</i> , 4562–4578
2		<i>J. Med. Chem.</i> 2020 , <i>63</i> , 4562–4578
3		<i>J. Med. Chem.</i> 2020 , <i>63</i> , 4562–4578
4		<i>J. Med. Chem.</i> 2020 , <i>63</i> , 4562–4578
5		<i>J. Med. Chem.</i> 2020 , <i>63</i> , 4562–4578
6		<i>J. Med. Chem.</i> 2020 , <i>63</i> , 4562–4578
7		<i>J. Med. Chem.</i> 2020 , <i>63</i> , 4562–4578
8		<i>J. Med. Chem.</i> 2020 , <i>63</i> , 4562–4578
9		<i>J. Med. Chem.</i> 2020 , <i>63</i> , 4562–4578

10		<i>J. Med. Chem.</i> 2020 , <i>63</i> , 4562–4578
11		<i>J. Med. Chem.</i> 2020 , <i>63</i> , 4562–4578
12		<i>ACS Med. Chem. Lett.</i> 2020 , <i>11</i> , 2526–2533
13		<i>ACS Med. Chem. Lett.</i> 2020 , <i>11</i> , 2526–2533
14		<i>ACS Med. Chem. Lett.</i> 2020 , <i>11</i> , 2526–2533
15		<i>ACS Med. Chem. Lett.</i> 2020 , <i>11</i> , 2526–2533
16		<i>ACS Med. Chem. Lett.</i> 2020 , <i>11</i> , 2526–2533
17		<i>ACS Med. Chem. Lett.</i> 2020 , <i>11</i> , 2526–2533
18		<i>ACS Med. Chem. Lett.</i> 2020 , <i>11</i> , 2526–2533
19		<i>Sci. Adv.</i> 2020 , <i>6</i> , eabe0751
20		<i>Sci. Adv.</i> 2020 , <i>6</i> , eabe0751

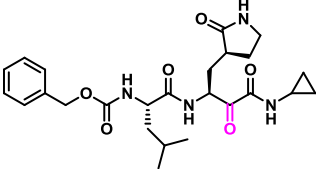
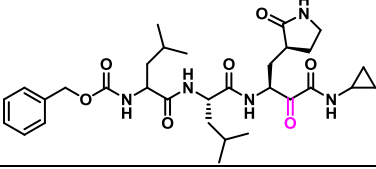
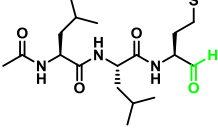
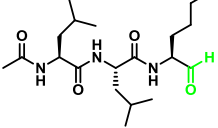
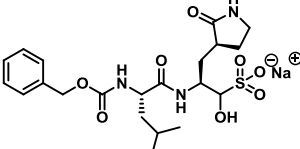
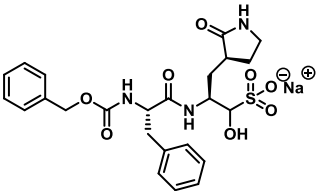
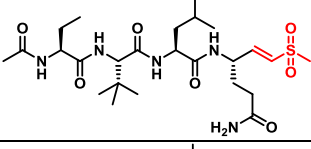
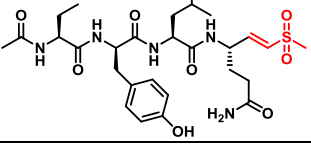
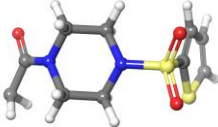
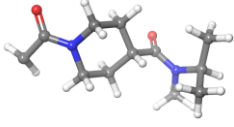
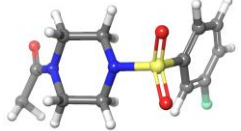
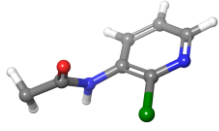
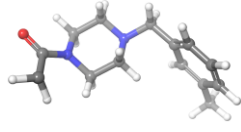

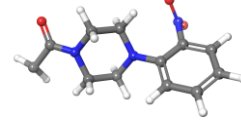

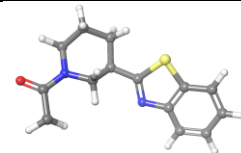

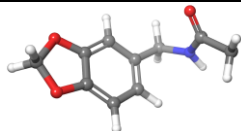
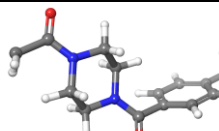
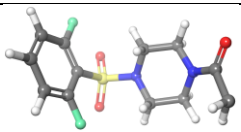
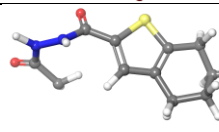
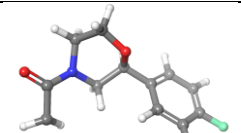
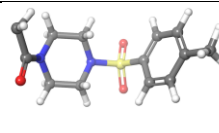

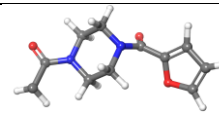
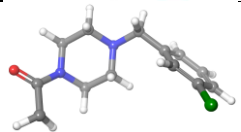
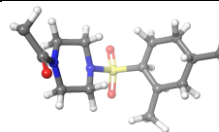
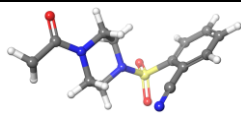

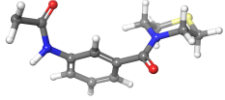
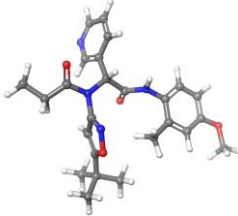
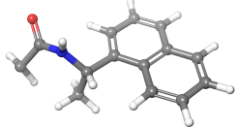
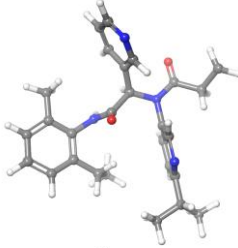
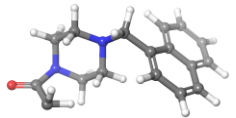
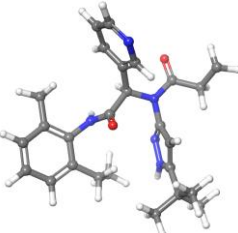
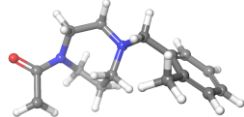
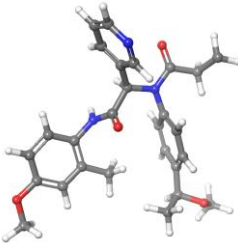
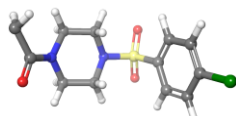
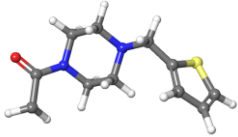

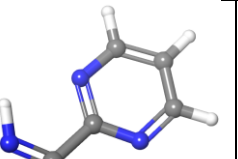
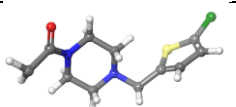
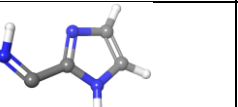
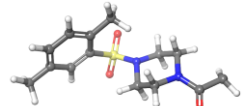
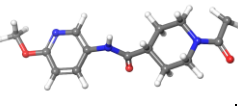
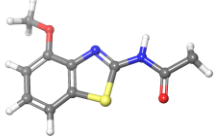

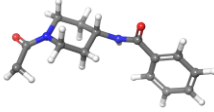
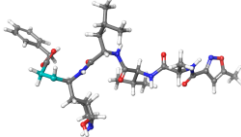
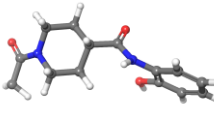
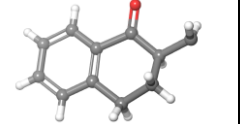
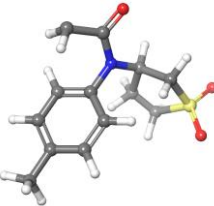
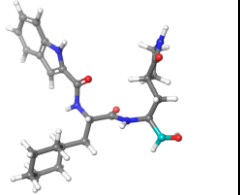
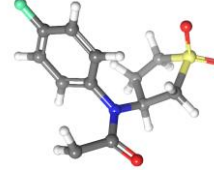
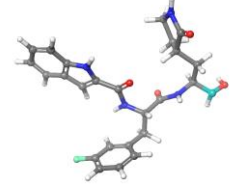
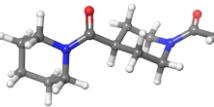
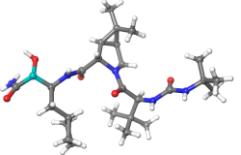
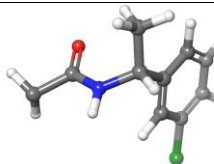
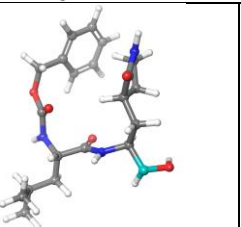
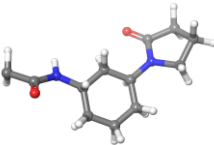
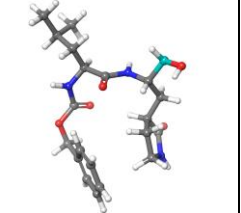
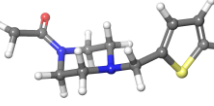
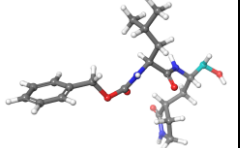
21		<i>Sci. Adv.</i> 2020 , <i>6</i> , eabe0751
22		<i>Sci. Adv.</i> 2020 , <i>6</i> , eabe0751
23		<i>Sci. Adv.</i> 2020 , <i>6</i> , eabe0751
24		<i>Sci. Adv.</i> 2020 , <i>6</i> , eabe0751
25		<i>Sci. Adv.</i> 2020 , <i>6</i> , eabe0751
26		<i>Sci. Adv.</i> 2020 , <i>6</i> , eabe0751
27		<i>Nat Chem Biol</i> , 2020 , https://doi.org/10.1038/s41589-020-00689-z
28		<i>Nat Chem Biol</i> , 2020 , https://doi.org/10.1038/s41589-020-00689-z

Table S4: Binding energy (ΔG) of ligands found in active site of SARS-CoV-2 M^{pro} enzyme through covalent bond.

Entry	PDB id	Ligand	ΔG (KJ/mol)	Entry	PDB id	Ligand	ΔG (KJ/mol)
1.	5REJ		-24.94	35	5RFY		-19.28

2.	5REK		-26.92	36	5RFZ		-15.92
3.	5REL		-25.24	37	5RG0		-14.66
4.	5REM		-21.71	38	5RG2		-12.55
5.	5REN		-23.39	39	5RG3		-10.25
6.	5REO		-21.50	40	5RGL		-27.26
7.	5REP		-24.74	41	5RGM		-23.05
8.	5RER		-24.36	42	5RGN		-28.10
9.	5RES		-24.25	43	5RGO		-25.99
10	5RET		-21.38	44	5RGP		-17.59
11	5REU		-21.21	45	5RGT		-30.61

12	5REV		-28.06	46	5RH5		-31.21
13	5REW		-25.28	47	5RH6		-34.82
14	5REX		-29.82	48	5RH7		-34.39
15	5REY		-28.09	49	5RH9		-33.35
16	5RFF		-25.99	50	5RHA		-24.95
17	5RFG		-23.89	51	5RHB		-12.34
18	5RFH		-23.14	52	5RHC		-11.97
19	5RFI		-24.95	53	5RHE		-22.89

20	5RFJ		-17.26	54	5RHF		-23.86
21	5RFK		-20.45	55	6LU7		-8.86
22	5RFL		-20.66	56	6YNQ		-13.06
23	5RFM		-23.98	57	6LZE		-29.61
24	5RFN		-24.31	58	6MOK		-29.86
25	5RFO		-17.34	59	6WNP		-8.61
26	5RFP		-18.94	60	6WTJ		-12.39
27	5RFQ		-19.70	61	6WTK		-12.10
28	5RFR		-26.25	62	6WTM		-12.51

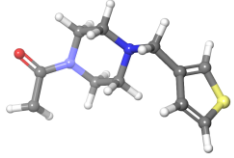
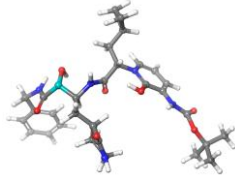
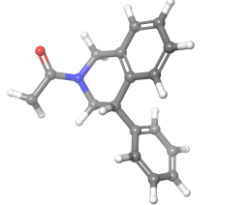
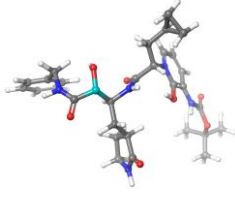
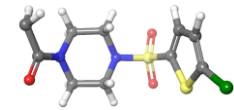
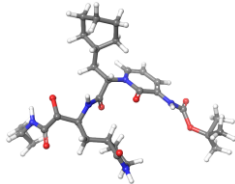
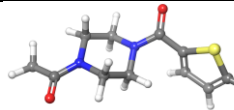
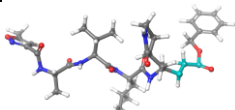
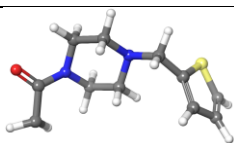
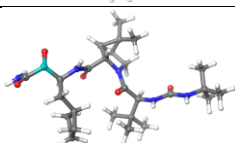
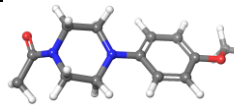
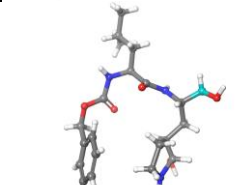
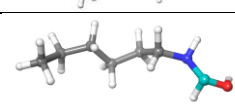
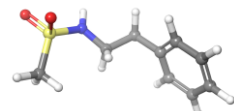
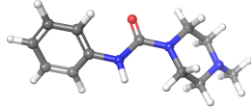
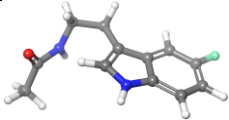
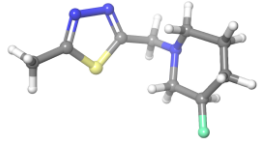
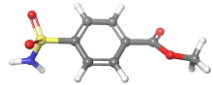
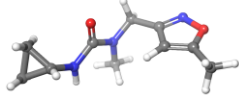
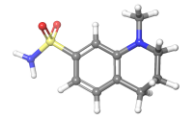
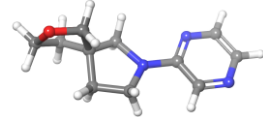
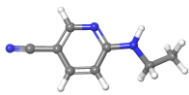
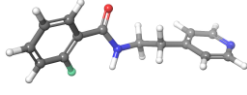
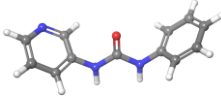
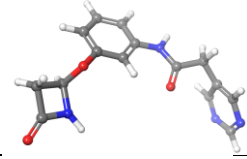
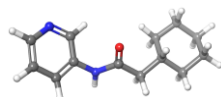
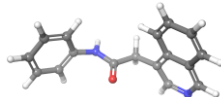
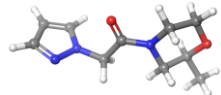
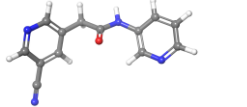
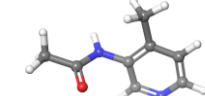
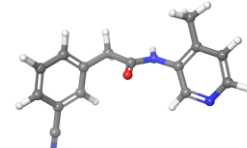
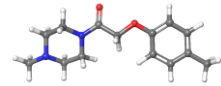
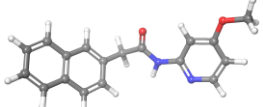
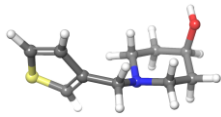
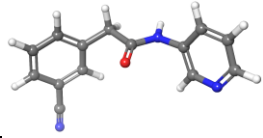
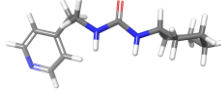
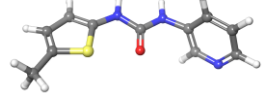
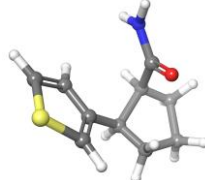
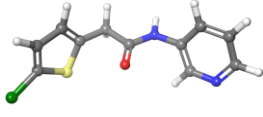
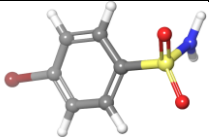
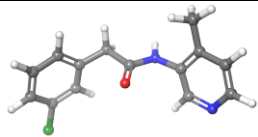
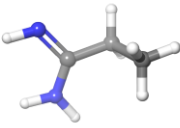
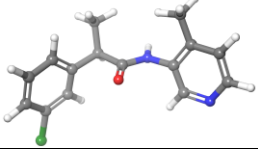

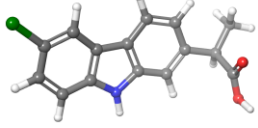
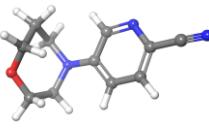
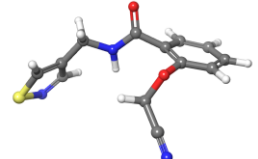
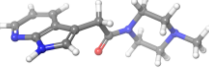
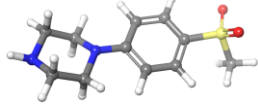
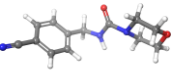
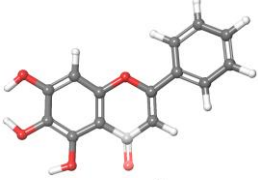
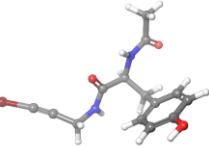
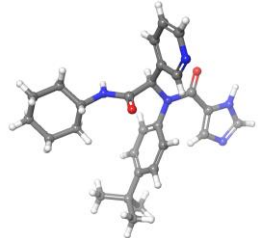
29	5RFS		-26.96	63	6Y2F		-11.80
30	5RET		-28.14	64	6Y2G		-1138
31	5REU		-22.76	65	6Y7M		-16.59
32	5REV		-21.50	66	7BQY		-15.58
33	5RFW		-21.29	67	7BRP		-12.22
34	5RFX		-23.48	68	7BRR		-16.00
				69	7BUY		-7.60

Table S5: Binding energy (ΔG) of ligands found in active site of SARS-CoV-2 M^{pro} enzyme through non-covalent bond.

Entry	PDB Id	Ligand	ΔG (KJ/mol)	Entry	PDB Id	Ligand	ΔG (KJ/mol)
1	5R7Y		-18.94	21	5RGG		-23.73

2	5R7Z		-20.83	22	5RGH		-21.42
3	5R80		-18.10	23	5RGI		-23.44
4	5R81		-22.26	24	5RGJ		-23.05
5	5R82		-22.09	25	5RGK		-24.31
6	5R83		-24.94	26	5RGU		-20.12
7	5R84		-21.92	27	5RGV		-28.52
8	5R89		-19.53	28	5RGW		-25.99
9	5RE4		-18.44	29	5RGX		-28.48
10	5RE9		-26.84	30	5RGY		-25.91
11	5REB		-24.69	31	5RGZ		-27.84
12	5REH		-25.07	32	5RH0		-25.75
13	5REZ		-23.98	33	5RH1		-26.25

14	5RF1		-21.42	34	5RH2		-26.75
15	5RF2		-4.62	35	5RH3		-26.96
16	5RF3		-10.96	36	5RH4		-27.89
17	5RF6		-23.44	37	5RH8		-25.49
18	5RF7		-28.06	38	5RHD		-24.02
19	5REE		-24.28	39	6M2 N		-26.50
20	5RG1		-20.08	40	6W63		-29.06